molbank

MDPI

Short Note

6-[(2*S*,3*R*)-3-(2,4-Difluorophenyl)-3-hydroxy-4-(1*H*-1,2,4-triazol-1-yl)butan-2-yl]-5-fluoropyrimidine-4-carbaldehyde

Joana L. C. Sousa *, Hélio M. T. Albuquerque * and Artur M. S. Silva

LAQV-REQUIMTE, Department of Chemistry, University of Aveiro, 3810-193 Aveiro, Portugal
* Correspondence: joanasousa@ua.pt (J.L.C.S.); helio.albuquerque@ua.pt (H.M.T.A.)

Abstract: Voriconazole (**VN**) is an antifungal drug indicated for the treatment of several fungal infections. Due to its side effects, some works involving late-stage functionalization of **VN** have been reported in the literature. Here, we disclose a new **VN** derivative, the 6-[(2*S*,3*R*)-3-(2,4-difluorophenyl)-3-hydroxy-4-(1*H*-1,2,4-triazol-1-yl)butan-2-yl]-5-fluoropyrimidine-4-carbaldehyde (**VN-CHO**). This compound results from the photoredox-catalyzed hydroxymethylation of **VN**, affording a hydroxymethylated derivative (**VN-CH_2OH**), followed by oxidation of the former CH_2OH group. **VN-CHO** was obtained in good yield (70% yield) and its structure was unveiled by 1D (^{1}H and ^{13}C) and 2D (HSQC and HMBC) NMR techniques. The introduction of a formyl group in **VN** structure creates a very promising site for further functionalization in a molecule which originally does not have many active sites.

Keywords: voriconazole; late-stage functionalization; hydroxymethylation; photoredox reaction; oxidation; NMR spectroscopy

check for updates

Citation: Sousa, J.L.C.; Albuquerque, H.M.T.; Silva, A.M.S. 6-[(2*S*,3*R*)-3-(2,4-Difluorophenyl)-3-hydroxy-4-(1*H*-1,2,4-triazol-1-yl)butan-2-yl]-5-fluoropyrimidine-4-carbaldehyde. *Molbank* **2023**, *2023*, M1603. https://doi.org/10.3390/M1603

Received: 6 February 2023
Revised: 15 February 2023
Accepted: 21 February 2023
Published: 12 March 2023

1. Introduction

Voriconazole (**VN**) is a well-known antifungal drug used to treat several fungal infections such as aspergillosis, candidiasis, coccidioidomycosis, histoplasmosis and penicilliosis, acting on fungal metabolism and fungal cell membranes. **VN** is the second generation of triazole antifungal drugs, derived from the former fluconazole (**FN**), both developed by Pfizer in the 1990s and 1980s, respectively, of the 20th century. Despite the good *in vivo* efficacy and excellent pharmacokinetic properties, invasive aspergillosis showed some resistance to **FN** [1–3]. The replacement of one triazole moiety in **FN** with a 5-fluoropyrimidine alongside the installation of a methyl group on the linker next to the stereogenic center ended up with **VN** (Figure 1). These structural modifications have been demonstrated to be quite favorable against all *Aspergillus* species, allowing to overcome the resistance associated with **FN**. Indeed, the **VN** showed to be 20-fold more potent against *Candida albicans* and *Candida glabrata* [4]. Over the years, **VN** was subjected to several other structural modifications, especially in the 5-fluoropyrimidine moiety, to favour its antifungal activity in terms of the enhancement of pharmacokinetic properties as well as to achieve tolerable toxicity profiles [5].

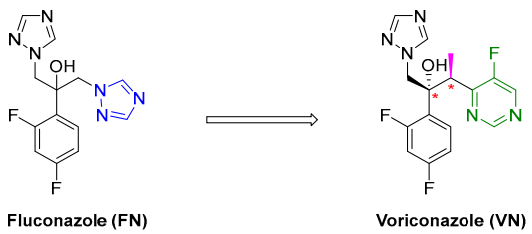

Figure 1. Second-generation triazole drug **VN**, derived from **FN**.

The stereochemical feature of **VN** is crucial for its potent antifungal activity. The installation of two contiguous chiral centers can be quite a challenge for synthetic chemists and therefore, it is very important to establish efficient enantioselective synthetic methods to prepare the **VN**. To the best of our knowledge, there are two main synthetic pathways for the synthesis of **VN** (see SI for details) [6,7].

The first synthetic route of **VN** involves five reaction steps (Scheme S1): (i) the Friedel-Crafts acylation of difluorobenzene with chloroacetyl chloride for the preparation of the 2-chloroacetophenone; (ii) the reaction of the 2-chloroacetophenone with 4-aminotriazole, followed by (iii) deamination to install the triazole moiety; (iv) installation of the pyrimidine moiety through the reaction of the organozinc reagent of 4-(1-bromoethyl)pyrimidine and the triazole ketone precursor (with the desired diastereoselectivity (2*R*,3*S*) over the (2*R*,3*R*)-isomer in a 12:1 ratio); and (v) catalytic hydrogenolysis in the presence of sodium acetate to give **VN** [6].

The second route towards **VN** differs from the previous one only in the final steps (Scheme S2). This means that the triazole ketone reacts with 4-chloro-6-ethyl-5-fluoropyrimidine upon deprotonation with lithium diisopropylamide (LDA) as a base in tetrahydrofuran (THF) at a low temperature, resulting in a 1:1 mixture of diastereomers (2*R*,3*S*)/(2*R*,3*R*). The final hydrogenolysis step requires an additional resolution step in order to obtain **VN**, limiting the synthetic utility of this route [7].

Given the synthetic difficulties of the enantioselective synthesis of **VN**, it is advisable for medicinal chemists the utilization of late-stage functionalization (LSF) methods, which use the C–H bonds of drug leads as points of diversification for generating new analogs. LSF approaches (Figure 2) offer interesting advantages such as the quick assessment of structure–activity relationships (SARs), optimization of on-target potency, selectivity and absorption–distribution–metabolism–excretion (ADME) properties, improvement of physical properties such as solubility and stability, the generation of oxidized metabolites, the blocking of metabolic hot spots as well as the preparation of biological probes, without resorting for arduous *de novo* chemical synthesis [8,9].

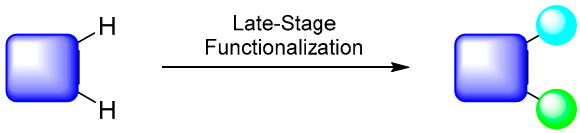

Figure 2. LSF operates C–H functionalization chemistries to directly modify lead structures, providing new analogs without resorting to *de novo* synthesis.

Within the LSF toolbox, several C–H functionalization reactions have been reported such as borylation, halogenation, oxidation and carbon–carbon bond formation reactions. One of the most important is perhaps the photoredox catalysis which enabled the development of completely new reaction mechanisms, facilitating the construction of challenging carbon–carbon and carbon–heteroatom bonds [10]. The installation of the hydroxymethyl group (-CH_2OH) is often desirable as it can modulate physical properties and solubility, and through hydrogen-bonding interactions, the binding mode of the pharmacophore. However, the hydroxymethyl is not the primer functional group for the generation of other target compounds. Luckily, this primary alcohol could be oxidized to its corresponding aldehyde, creating an appealing point of lead diversification through aldol reaction, Wittig reaction, imine formation, reductive amination and so on.

Herein, we installed a formyl group at C-4 of the pyrimidine unit of **VN** through oxidation of its hydromethylated precursor (**VN-CH_2OH**), which was obtained by photoredox-catalyzed hydroxymethylation of **VN** (Scheme 1).

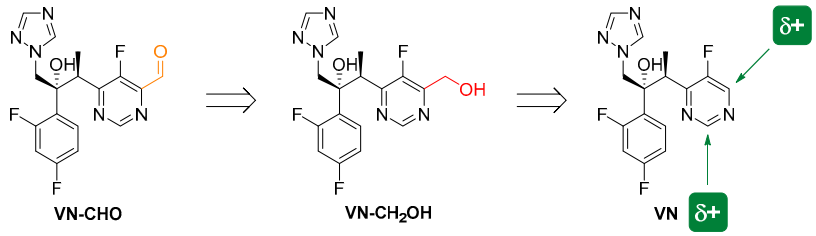

Scheme 1. Retrosynthetic analysis of the 6-[(2*S*,3*R*)-3-(2,4-difluorophenyl)-3-hydroxy-4-(1*H*-1,2,4-triazol-1-yl)butan-2-yl]-5-fluoropyrimidine-4-carbaldehyde (**VN-CHO**), starting from **VN**.

2. Results and Discussion

Firstly, **VN** was converted into **VN-CH$_2$OH** through a photoredox-catalyzed hydroxymethylation procedure. This methodology consisted in the generation of hydroxymethyl radicals from methanol and their addition to **VN** using a photoredox approach [11]. To do so, we used an irradiation source based on blue LEDs in the presence of an Ir(III)-photocatalyst–[Ir(dF-CF$_3$-ppy)$_2$(dtbpy)]PF$_6$–and benzoyl peroxide (BPO) as oxidant (Scheme 2). The desired hydroxymethylated **VN** (**VN-CH$_2$OH**) was obtained together with a byproduct resulting from the dihydroxymethylation of **VN** at C-2 and C-4 of the pyrimidine ring [**VN-(CH$_2$OH)$_2$**].

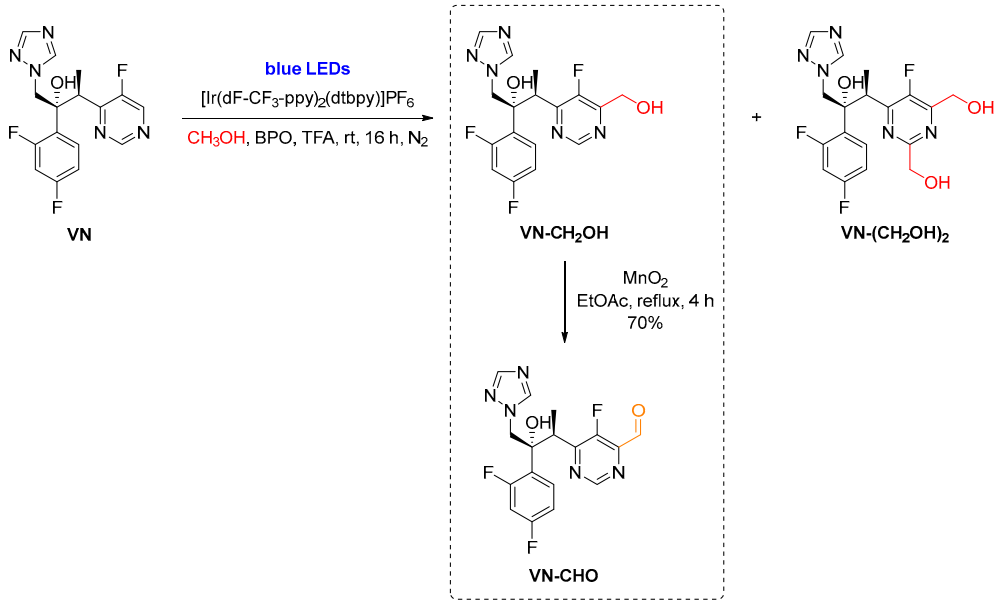

Scheme 2. Synthesis of the 6-[(2*S*,3*R*)-3-(2,4-difluorophenyl)-3-hydroxy-4-(1*H*-1,2,4-triazol-1-yl)butan-2-yl]-5-fluoropyrimidine-4-carbaldehyde (**VN-CHO**).

Next, **VN-CH$_2$OH** was oxidized to **VN-CHO** in the presence of activated manganese dioxide as an oxidizing agent (Scheme 2). Using an excess of MnO$_2$, in ethyl acetate, at reflux for 4 h, **VN-CHO** was obtained in 70% yield. It is noteworthy that this methodology is regioselective as the hydroxymethylation step occurs predominantly at C-4 of the pyrimidine ring of **VN** and consequently, only one regioisomer was obtained. On the other hand, if a standard Vilsmeier–Haack formylation procedure was performed directly in the **VN**, the desired **VN-CHO** might not be obtained since the preferred sites for formylation would be the electron-rich 1,2,4-triazole and difluorophenyl moieties (Figure 3).

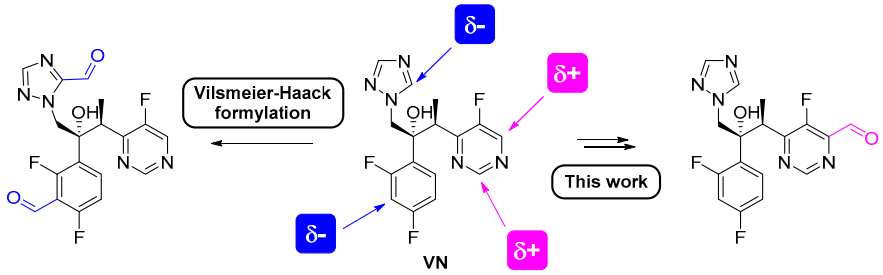

Figure 3. Hypothetical Vilsmeier–Haack formylation sites versus this regioselective two-step methodology.

VN-CHO was fully characterized by 1D (^{1}H and ^{13}C) (Figures S1 and S2) and 2D (HSQC and HMBC) (Figures S3 and S4) NMR techniques. In its ^{1}H NMR spectrum (Figure S1), the most characteristic signals are:

(i) The doublet ($J_{H\text{-}F}$ 0.6 Hz) at δ_H 10.19 ppm, which corresponds to the resonance of the proton of the 4-C*H*O group.
(ii) The doublet ($J_{H\text{-}F}$ 1.6 Hz) at δ_H 9.08 ppm, which corresponds to the resonance of H-2 of the pyrimidine ring.
(iii) Two singlets at δ_H 7.54 and 7.96 ppm, which correspond to the resonance of H-3′′′ and H-5′′′ of the 1,2,4-triazole moiety.
(iv) The broad singlet at δ_H 6.19 ppm, which corresponds to the resonance of the proton of the 3′-O*H* group.
(v) The doublet ($J_{1'\text{-}2'}$ 7.1 Hz) at δ_H 1.15 ppm, which corresponds to the resonance of the protons of the 2′-CH_3 group.

In addition, through the observed correlations in the HMBC spectrum of **VN-CHO** (Figure S4), we were able to unequivocally assign all nonprotonated carbons (Figure 4):

(i) C-4 (δ_c 144.2 ppm) as a doublet ($^{2}J_{4\text{-}F}$ 7.0 Hz) due to its connectivities with 4-C*H*O and H-2.
(ii) C-5 (δ_c 153.8 ppm) as a doublet ($^{1}J_{5\text{-}F}$ 282.3 Hz) due to its connectivities with 4-C*H*O and H-2′.
(iii) C-6 (δ_c 163.6 ppm) as a doublet ($^{2}J_{6\text{-}F}$ 13.3 Hz) due to its connectivities with H-2, H-2′ and 2′-CH_3.
(iv) C-3′ (δ_c 77.6 ppm) due to its connectivities with 2′-CH_3, H-2′, H-4′ and H-6′′.
(v) C-1′′ (δ_c 123.4 ppm) as a doublet of doublets ($^{4}J_{1''\text{-}F}$ 4.0 and $^{2}J_{1''\text{-}F}$ 12.3 Hz) due to its connectivities with 3′-O*H*, H-4′, H-3′′ and H-5′′.
(vi) C-2′′ and C-4′′ (δ_c 156.7–164.6 ppm) due to its connectivities with H-6′′. However, their signals are hidden by the background noise in the ^{13}C NMR spectrum, which prevented their accurate assignment.

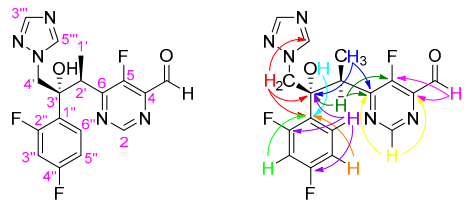

Figure 4. Numbering system and main HMBC connectivities observed in the HMBC spectrum of **VN-CHO**.

3. Materials and Methods

3.1. General Remarks

Melting points were measured with a Büchi Melting Point B-540 apparatus and are uncorrected. NMR spectra were recorded with a Bruker Avance 300 spectrometer (300 MHz

for ^{1}H and 75 MHz for ^{13}C), in $CDCl_3$ as solvent. Chemical shifts are reported in ppm and coupling constants (*J*) in Hz; the internal standard was tetramethylsilane (TMS). Unequivocal ^{13}C assignments were made with the aid of 2D *g*HSQC and *g*HMBC (delays for one-bond and long-range *J* C/H couplings were optimized for 145 and 7 Hz, respectively) experiments. Positive ESI mass spectra were acquired with a QTOF 2 spectrometer. Preparative thin layer chromatography (TLC) was performed with Macherey–Nagel silica gel G/UV254. All chemicals and solvents were obtained from commercial sources and used as received or dried by standard procedures. **VN** was obtained by liquid–liquid extraction of the lyophilized powder of Vfend® for intravenous infusion provided by the Hospital de Santa Maria, Lisbon, Portugal. **VN-CH$_2$OH** was synthesized according to a procedure described in the literature [11].

*3.2. General Procedure for the Synthesis of 6-[(2S,3R)-3-(2,4-Difluorophenyl)-3-hydroxy-4-(1H-1,2,4-triazol-1-yl)butan-2-yl]-5-fluoropyrimidine-4-carbaldehyde (**VN-CHO**)*

MnO_2 (349 mg; 4.02 mmol) was added to a solution of **VN-CH$_2$OH** (127 mg; 0.335 mmol) in EtOAc (6 mL). The reaction mixture was stirred at reflux for 4 h. After this time, the reaction mixture was filtered through a celite pad and then, the reaction crude was purified by preparative TLC using a mixture of 5% MeOH/CH_2Cl_2 as eluent. **VN-CHO** was obtained as a white solid (88.5 mg, 70% yield). Mp 91–94 °C. ^{1}H NMR (300 MHz, $CDCl_3$): δ 1.15 (d, *J* 7.1 Hz, 3H, 2′-C*H*$_3$), 4.22–4.29 (m, 1H, H-2′), 4.40 and 4.73 (2 d, *J* 14.2 Hz, 2H, H-4′), 6.19 (br s, 1H, 3′-O*H*), 6.80–6.91 (m, 2H, H-3′′,5′′), 7.54 (s, 1H, H-3′′′), 7.64 (dt, *J* 6.6 and 9.2 Hz, 1H, H-6′′), 7.96 (s, 1H, H-5′′′), 9.08 (d, *J* 1.6 Hz, H-2), 10.19 (d, *J* 0.6 Hz, 1H, 4-C*H*O) ppm. ^{13}C NMR (75 MHz, $CDCl_3$): δ 16.1 (2′-CH_3), 37.6 (d, *J* 5.2 Hz, C-2′), 57.1 (d, *J* 5.4 Hz, C-4′), 77.6 (C-3′), 104.3 (dd, *J* 25.8 and 27.5 Hz, C-3′′), 111.8 (dd, *J* 3.4 and 20.6 Hz, C-5′′), 123.4 (dd, *J* 4.0 and 12.3 Hz, C-1′′), 130.6 (dd, *J* 5.6 and 9.5 Hz, C-6′′), 144.1 (C-5′′′), 144.2 (d, *J* 7.0 Hz, C-4), 151.2 (C-3′′′), 153.5 (d, *J* 9.9 Hz, C-2), 153.8 (d, *J* 282.3 Hz, C-5), 163.6 (d, *J* 13.3 Hz, C-6), 188.4 (d, *J* 2.2 Hz, 4-CHO) ppm. HRMS-ESI$^+$ *m/z* calcd for [$C_{17}H_{14}F_3N_5O_2$ + CH_3OH + H]$^+$: 410.1440, found: 410.1435.

4. Conclusions

In conclusion, we synthesized a new **VN** derivative employing a LSF approach. **VN-CHO** was obtained in good yield through a regioselective methodology, which involved a photoredox-catalyzed hydroxymethylation reaction followed by an oxidation step with manganese dioxide. The installation of the formyl group occurred at C-4 of the pyrimidine ring of **VN**, creating a new active site for further functionalization through many well-known transformations involving aldehydes (for instance, Witting reaction, aldol condensation, reductive amination, among others).

Supplementary Materials: The following supporting information can be downloaded online, Scheme S1: First synthetic route for the synthesis of Voriconazole (**VN**); Scheme S2: Second synthetic route for the synthesis of Voriconazole (**VN**); Figure S1: ^{1}H NMR spectrum of the title compound (**VN-CHO**); Figure S2: ^{13}C NMR spectrum of the title compound (**VN-CHO**); Figure S3: HSQC spectrum of the title compound (**VN-CHO**); Figure S4: HMBC spectrum of the title compound (**VN-CHO**); Figure S5: HRMS spectrum of the title compound (**VN-CHO**).

Author Contributions: Conceptualization, methodology, investigation, and writing—original draft preparation, J.L.C.S. and H.M.T.A.; writing—review and editing, supervision, and project administration, A.M.S.S. All authors have read and agreed to the published version of the manuscript.

Funding: This work received financial support from PT national funds (FCT/MCTES, Fundação para a Ciência e a Tecnologia and Ministério da Ciência, Tecnologia e Ensino Superior) through the project LAQV-REQUIMTE (UIDB/50006/2020 and UIDP/50006/2020), as well as the Portuguese NMR Network. Joana Sousa gratefully acknowledges LAQV-REQUIMTE for her researcher contract.

Data Availability Statement: Not applicable.

Acknowledgments: The authors would like to thank René Santus, Emeritus Professor, from the Muséum National d'Histoire Naturelle, Paris, France, and Hospital de Santa Maria, Lisbon, Portugal, for kindly provide Vfend®.

Conflicts of Interest: The authors declare no conflict of interest.

References

1. Arendrup, M.C. Update on antifungal resistance in Aspergillus and Candida. *Clin. Microbiol. Infect.* **2014**, *20*, 42–48. [CrossRef] [PubMed]
2. Ding, Z.; Ni, T.; Xie, F.; Hao, Y.; Yu, S.; Chai, X.; Jin, Y.; Wang, T.; Jiang, Y.; Zhang, D. Design, synthesis, and structure-activity relationship studies of novel triazole agents with strong antifungal activity against Aspergillus fumigatus. *Bioorg. Med. Chem. Lett.* **2020**, *30*, 126951. [CrossRef] [PubMed]
3. Garcia-Effron, G. Molecular Markers of Antifungal Resistance: Potential Uses in Routine Practice and Future Perspectives. *J. Fungi* **2021**, *7*, 197. [CrossRef] [PubMed]
4. Shafiei, M.; Peyton, L.; Hashemzadeh, M.; Foroumadi, A. History of the development of antifungal azoles: A review on structures, SAR, and mechanism of action. *Bioorg. Chem.* **2020**, *104*, 104240. [CrossRef] [PubMed]
5. Ghobadi, E.; Saednia, S.; Emami, S. Synthetic approaches and structural diversity of triazolylbutanols derived from voriconazole in the antifungal drug development. *Eur. J. Med. Chem.* **2022**, *231*, 114161. [CrossRef] [PubMed]
6. Butters, M.; Ebbs, J.; Green, S.P.; MacRae, J.; Morland, M.C.; Murtiashaw, C.W.; Pettman, A.J. Process Development of Voriconazole: A Novel Broad-Spectrum Triazole Antifungal Agent. *Org. Process Res. Dev.* **2001**, *5*, 28–36. [CrossRef]
7. Sundaram, D.T.S.S.; Mitra, J.; Islam, A.; Prabahar, K.J.; Venkateswara Rao, B.; Paul Douglas, S. Synthesis of Isomeric and Potent Impurities of the Triazole-Based Antifungal Drug Voriconazole. *Sci. Pharm.* **2015**, *83*, 445–452. [CrossRef] [PubMed]
8. Moir, M.; Danon, J.J.; Reekie, T.A.; Kassiou, M. An overview of late-stage functionalization in today's drug discovery. *Expert Opin. Drug Discov.* **2019**, *14*, 1137–1149. [CrossRef] [PubMed]
9. Cernak, T.; Dykstra, K.D.; Tyagarajan, S.; Vachal, P.; Krska, S.W. The medicinal chemist's toolbox for late stage functionalization of drug-like molecules. *Chem. Soc. Rev.* **2016**, *45*, 546–576. [CrossRef] [PubMed]
10. Shaw, M.H.; Twilton, J.; MacMillan, D.W.C. Photoredox Catalysis in Organic Chemistry. *J. Org. Chem.* **2016**, *81*, 6898–6926. [CrossRef]
11. Huff, C.A.; Cohen, R.D.; Dykstra, K.D.; Streckfuss, E.; DiRocco, D.A.; Krska, S.W. Photoredox-Catalyzed Hydroxymethylation of Heteroaromatic Bases. *J. Org. Chem.* **2016**, *81*, 6980–6987. [CrossRef]